# Fourier-transform radiation thermometry: measurements and uncertainties

Pierre C. Dufour, Nelson L. Rowell, and Alan G. Steele

A Fourier-transform radiometer is used to measure blackbody temperatures in the 500–1000-K range. The measurements involve collecting mid-infrared spectra at two known reference temperatures and one unknown temperature. The accuracy of the interpolation measurement technique is discussed, and the effects of the uncertainty in the temperature reference points, the voltage ratio measurement, and the wavelength accuracy are described. Temperature accuracy at the 0.5% level has been achieved; the main uncertainty component is caused by the interferometer drift. Directions to reach 100-mk accuracy levels have been identified.

*OCIS codes:* 120.5636, 120.6780, 120.6200, 300.2140, 300.6300, 300.6340.

## 1. Introduction

Optical temperature-sensing techniques constitute a rapidly growing field. Compared with conventional temperature-measurement techniques, optical temperature measurement has the advantage of being noncontact, and the optical thermometer thus can be remote from the object under investigation. For that reason, optical thermometry has great utility for temperature measurement in corrosive or otherwise adverse environments and can be the only practical technique if the unknown temperature source cannot be reached.

Although the current state of the art for accurate optical temperature measurements relies on cryogenic radiometers,[1,2] such devices are generally not used in the infrared. Michelson-type interferometers for use from 2.5 to 25 μm have been developing quickly, owing to their portability, ease of operation, good resolution, high wavelength accuracy, and high throughput.[3] Radiance measurements with Michelson-type instruments have applications in atmospheric research,[4] emissivity measurements,[5–7] pollution characterization,[8] microwave background temperature measurement,[9] and moving particle temperature measurement.[10] Interferometer calibration has also been explored in Ref. 11. Furthermore, Gebbie *et al.*[12] and Gebbie[13] have suggested that it may be possible to define a temperature scale in terms of a wavelength standard by use of a Fourier-transform spectrometer output signal.

We present one of the basic temperature-interpolation schemes and discuss, theoretically and experimentally, the accuracy of the technique. The proposed technique has the potential for high accuracy and could provide important calibration capabilities. Here the major issue is the measurement accuracy that can be achieved with a Michelson interferometer.

## 2. Theory

The basis for optical temperature measurement is Planck's radiation law, which states that the radiance, $L_{\text{Planck}}$, of a blackbody (i.e., a medium absorbing all radiation incident upon it) in equilibrium at a temperature $T$ is given by

$$L_{\text{Planck}}(\nu, T) = \frac{c_1 \nu^3}{\exp(c_2 \nu / T) - 1}, \tag{1}$$

where $\nu$ is the wave-number value of the radiation emitted and $c_1$ and $c_2$ are the first and the second radiation constants, respectively ($c_1 = 1.19106 \times 10^{-12}$ W cm$^2$/sr).[6] The wave-number value (also called frequency in this paper) is defined as the reciprocal of the vacuum wavelength in centimeters. In the International Temperature Scale of 1990 (ITS-90),[14] Planck's law is used to define the temperature above the freezing point of silver. Because we are ultimately interested in a comparison of our interpolation technique with accurate temperature measurement made according to the ITS-90 recom-

The authors are with the Institute for National Measurement Standards, National Research Council of Canada, Building M36, Montreal Road, Ottawa, Ontario K1A 0R6, Canada.

Received 6 February 1998; revised manuscript received 27 April 1998.

mendations, the value of $c_2$ defined by the ITS-90, i.e., 1.4388 K/cm$^{-1}$, will be used.

In practice, radiation sources are never perfect absorbers, and the temperature- and frequency-dependent emissivity,[15] $\varepsilon(\nu, T)$, is defined to link the radiance of a real source to that of a blackbody:

$$L(\nu, T) = \varepsilon(\nu, T) L_{\text{Planck}}(\nu, T). \tag{2}$$

A Fourier-transform spectrometer is expected to have a signal output $V(\nu, T)$ that is proportional to the source radiance $L(\nu, T)$, given by

$$V(\nu, T) = R(\nu)[L(\nu, T) + L_{\text{bckg}}(\nu)], \tag{3}$$

where $R(\nu)$ is the interferometer response and $L_{\text{bckg}}(\nu)$ is the spectrometer self-emission or background signal. In Fourier-transform spectroscopy the interferometer creates a wavelength-dependent modulation of the source intensity, and $V(\nu, T)$ is the Fourier transform of the signal ac component $V(x, T)$ that is produced by the radiation incident upon the detector. Inasmuch as the phase of the self-emitted radiation $L_{\text{bckg}}(\nu)$ and that of the source $L(\nu, T)$ are not necessarily the same,[4] either the quantities $R(\nu)$ and $L_{\text{bckg}}(\nu)$ must be treated as complex functions or the background must be removed before the Fourier transform is performed when conventional phase-correction techniques are used. The latter approach is used in this paper because it leads to a simpler uncertainty analysis. We eliminate the interferometer response and the background in a calibration procedure by measuring the interferometer output for two known blackbody temperatures, $T_1$ and $T_2$. It is useful to introduce the ratio of the measured signal difference, in this way removing the background and the spectrometer response from Eq. (3). However, we should compute the signal difference before the Fourier transform is performed to correct for a possible anomalous phase.[4] This leads to the following ratio function:

$$\begin{aligned} r &\equiv r(\nu, T, T_1, T_2) \\ &\equiv \frac{L(\nu, T) - L_{\text{Planck}}(\nu, T_1)}{L_{\text{Planck}}(\nu, T_2) - L_{\text{Planck}}(\nu, T_1)} \\ &\approx \frac{\Im[V(x, T) - V(x, T_1)]}{\Im[V(x, T_2) - V(x, T_1)]}, \end{aligned} \tag{4}$$

where $\Im$ is the Fourier transform and the various $V(x, T_k)$ are the measured interferograms. Even though we chose blackbodies for the reference radiance, any two sources of known radiance could have been used in the definition of $r$, except at frequencies where the two radiances are equal.

The derivation of the relation between the measured interferogram and the spectral radiant power assumes that the beam propagating in the interferometer is composed of plane waves. Even if diffraction and aberrations were neglected, this would be possible only for a point source placed at the collimator focal point. However, such a source would give zero radiant power, and in practice a finite source must be used. Furthermore, the Fourier integral can be only approximately realized: The actual data must be sampled, and the interferogram can be measured only up to a finite maximum path difference. This partial knowledge of the true continuous interferogram leads to known discrete Fourier-transform errors, such as aliasing, finite resolution, and leakage. Any detector nonlinearity is also expected to cause the last term of relation (4) to deviate from the defining radiance ratio. For all these reasons the experimental ratio will differ from the ratio definition. One of our goals is to examine the measurement accuracy and corrections in the last term of relation (4) that are necessary for temperature accuracy at the millikelvin level.

For an unknown temperature $T$ in the $[T_1, T_2]$ range, the function $r$ takes values between 0 and 1. Even though we chose to use it this way in this paper, the technique is not restricted to interpolation and can also be used if the unknown temperature is outside the $[T_1, T_2]$ interval. Relation (4) can be rearranged and used as an interpolation function for obtaining the unknown radiance:

$$L(\nu, T) = rL_2 + (1 - r)L_1, \tag{5}$$

where we have abbreviated $L_{\text{Planck}}(\nu, T_k)$ as $L_k$. Equation (5) has the advantage that the uncertainties in the reference temperatures spectra are well separated from the uncertainties in the voltage measurements.

In the case when the unknown temperature source is also a blackbody, its temperature is given by

$$T = c_2 \nu \Big/ \ln\left[\frac{c_1 \nu^3}{rL_2 + (1 - r)L_1} + 1\right]. \tag{6}$$

Because our spectra are measured over a broad spectral band, we can use Eq. (6) to obtain the temperature from the ratio at any and all of the measured frequencies. This spectral temperature function should be a constant for all wave numbers in the error-free case; any deviations provide us with information about the accuracy of the technique.

In the limit of monochromatic radiation, if $T_1$ is allowed to go to 0, and $T_2$ is taken to be the temperature of the freezing point of silver, gold, or copper, the expression for the voltage ratio [relation (4)] becomes identical to the ITS-90 definition of the temperature above the freezing point of silver.[14] Therefore it should be possible to modify the interpolation scheme to provide a realization of the ITS-90, once the uncertainties are well understood and under control.

There is, however, an important difference between the actual expression used and the ITS-90 defining expression, namely, the presence of the low-temperature reference point. The low-temperature reference is introduced because the 300-K background has significant magnitude relative to the measured signal and thus cannot be neglected: For example, at 180 cm$^{-1}$ the radiance ratio of a 500-K to

a 293-K blackbody is 2, and therefore the background correction term has the same magnitude as the measured signal. An alternative approach to relation (4) would be to define $r$ without the $L_1$ term and to use, for example, a low-temperature blackbody to measure the background and correct the ratio measurement, although this involves additional complications in the operation of the interferometer itself.

Because of the simple form of Eq. (6), the uncertainty analysis is straightforward. The natural independent variables for the uncertainty analysis are the measured quantities, namely, the three voltages and the two reference temperatures. However, the interpolated temperature depends on these five variables only through the radiance. Furthermore, the radiance depends on the voltages only through the experimental voltage ratio. Therefore it is possible to use the experimental ratio and the two reference temperatures as independent variables for the derived temperature or radiance. The propagation of uncertainty calculations is summarized below in Eqs. 7–10.

From Planck's law, the uncertainty in the derived temperature that is due to the uncertainty in the radiance is given by

$$\Delta T = \frac{T^2}{c_2 \nu}\left[1 - \exp\left(-\frac{c_2 \nu}{T}\right)\right]\frac{\Delta L}{L}, \tag{7}$$

and from the interpolation formula [Eq. (5)] the uncertainties in the radiance caused by an uncertainty in the reference temperatures and in the voltage ratio are given, respectively, by

$$\frac{\Delta L}{L} = \frac{(1-r)L_1}{rL_2 + (1-r)L_1}\frac{c_2 \nu}{T_1^2}\left[1 - \exp\left(-\frac{c_2 \nu}{T_1}\right)\right]^{-1}\Delta T_1, \tag{8}$$

$$\frac{\Delta L}{L} = \frac{rL_2}{rL_2 + (1-r)L_1}\frac{c_2 \nu}{T_2^2}\left[1 - \exp\left(-\frac{c_2 \nu}{T_2}\right)\right]^{-1}\Delta T_2, \tag{9}$$

$$\frac{\Delta L}{L} = \frac{L_2 - L_1}{L}\Delta r = \frac{L_2 - L_1}{(1-r)L_1 + rL_2}\Delta r. \tag{10}$$

We shall use these expressions later to discuss the uncertainty in the computed temperature that arises from the measurement uncertainties in voltage, wave number, and reference temperature.

### 3. Experiment

A diagram of the apparatus is shown in Fig. 1. It consists of (a) a variable-temperature blackbody radiator (Infrared Industries, Inc., Model 463), (b) a parabolic mirror acting as a collimator, (c) an aperture, and (d) a Bomem Michelson MB102 interferometer equipped with (e) a deuterated triglycine sulfate (DTGS) detector.

The interferometer windows and the beam splitter substrate are made of cesium iodide. This instrument covers the spectral range from 180 to roughly 5000 $cm^{-1}$. The beam path from the blackbody (a) to the interferometer port (g) is through ambient air, whereas the rest of the apparatus is enclosed in a dry air-purged box. The parabolic mirror (b) has a focal length of 50.8 mm, and its focal point is near the middle of the blackbody cavity, which is a 20°, 2-cm-long oxidized stainless-steel cone. Collimating in this way avoids imaging the hot ceramic tube at the front of the blackbody onto the aperture. The aperture (c) in the collimated beam is set to a size smaller than the diameter of the infrared beam (2 cm) at the interferometer entrance port (g). The detector area is 1 $mm^2$ and is the limiting aperture of the system. The blackbody temperature is measured with a type S (platinum 10% rhodium versus platinum) thermocouple. The uncertainty in the thermocouple voltage reading is 0.004 mV, corresponding to a temperature uncertainty of approximately 0.4 K, which is smaller than the thermocouple calibration uncertainty (0.7 K). Although the blackbody source is not of the highest quality, it is still useful for our initial investigation because we are interested in the application and development of the optical techniques and in understanding the Fourier-transform and other uncertainty components that affect our ability to determine the unknown temperature.

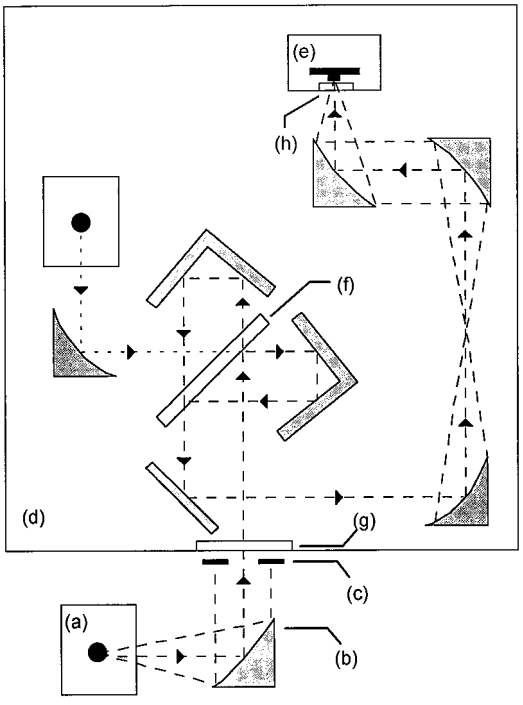


Fig. 1. Schematic of the apparatus: (a) blackbody; (b) collimator; (c) aperture; (d) interferometer; (e) DTGS detector; (f) beam splitter; (g), (h) windows.

### 4. Results

The data were acquired at a spectral resolution of 4 $cm^{-1}$ for source temperatures of 500–1000 K. The two extreme temperatures provide the reference spectra at $T_1$ and $T_2$, respectively, for the interpolation technique described in Section 2.

The first step in the analysis is to Fourier transform the appropriate interferogram differences and to compute the voltage ratios ($r$) according to relation

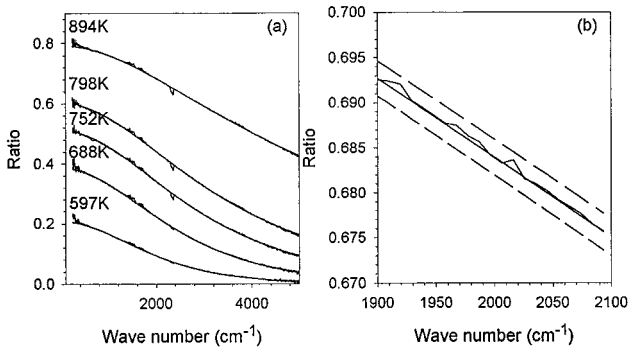


Fig. 2. (a) Experimental and theoretical values of the ratio function $r$ for $T_1 = 492.8$ K and $T_2 = 1000.0$ K. (b) Zoom on the 894-K curve with extremal values of the $r$ function for a 1-K shift of measured reference temperatures (dashed curves).

(4). The experimental values of the function $r$ are shown in Fig. 2(a) with the theoretical curves computed from relation (4) with the thermocouple temperature reading. Figure 2(b) shows the voltage ratio in a small spectral band near 2000 $cm^{-1}$ for the 894-K spectrum, together with the calculated extremal values of the ratio function for a 1-K shift of the assigned reference temperatures. The overall agreement between the two sets of curves is well within 1 K.

From these voltage ratios and Eq. (5) we can now compute the unknown temperature blackbody radiance curves, from which we extract the temperatures by using Eq. (6). The resultant temperature is illustrated as a function of wave number in Fig. 3. As can be seen, the observed deviations between the measured temperatures (from the thermocouple readings) and the average (over the 2400–2900-$cm^{-1}$ absorption free spectral window) derived temperatures are typically 0.5 K. The spectral bands, below 775 $cm^{-1}$, from 1150 to 2460 $cm^{-1}$, and from 2940 to 4210 $cm^{-1}$, are known to have significant atmospheric absorption, mainly from water vapor and $CO_2$. Concentration fluctuations of water vapor and $CO_2$ in the unpurged section of the optical path therefore lead to a large increase in the ratio (Fig. 2) and temperature (Fig. 3) uncertainty in those spectral bands. An obvious benefit of using the full spectrum is that the problem regions can readily be identified and taken out of the analysis. To improve on these results we must understand more about the origin of the uncertainties and the magnitude of each of the uncertainty components.

As discussed in Section 3, there is a 0.7-K uncertainty in each reference temperature from the calibration of the thermocouple and a supplementary 0.4-K uncertainty from the thermocouple voltage reading. In quadrature, these two sources of uncertainty sum to 0.8 K for the absolute uncertainty in each of $T_1$ and $T_2$. Combining Eq. (7) with Eqs. (8) and (9), we have all the information necessary to obtain the contribution of the uncertainty in the reference points to the temperature measurement uncertainty. The result is illustrated in Fig. 4, where

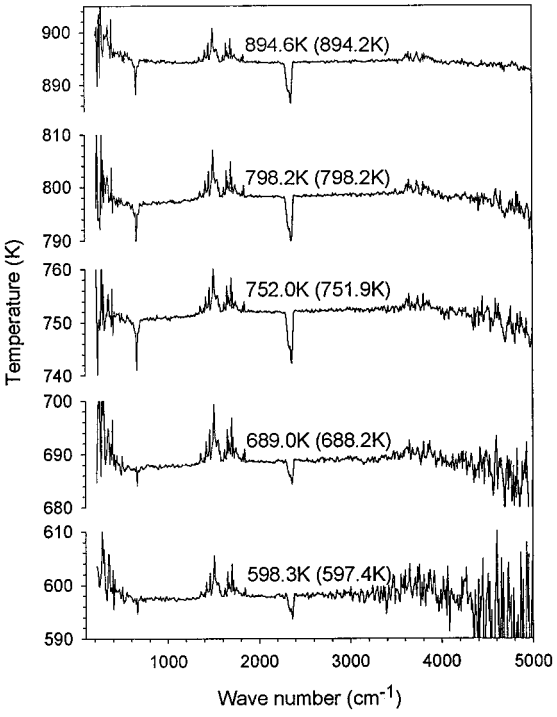


Fig. 3. Derived temperature versus wave number. The reference temperatures were $T_1 = 492.8$ K and $T_2 = 1000.0$ K. The calculated temperatures are indicated; measured thermocouple temperatures are shown in parentheses.

the temperature measurement uncertainty ($\Delta T$) is plotted as a function of wave number for various values of the temperature. The graph has been drawn to frequencies higher than the measurement limit to illustrate that at sufficiently high frequency the radiance of the low-temperature reference drops to a negligible level and the temperature uncertainty reaches the level given by the simpler expression in the ITS-90 supplementary information text,[16] with $T_2$ as the reference temperature.

For low-wave-number values the uncertainty is smallest near the average of the two reference temperatures. This behavior follows from the identical uncertainty on both reference temperatures and from

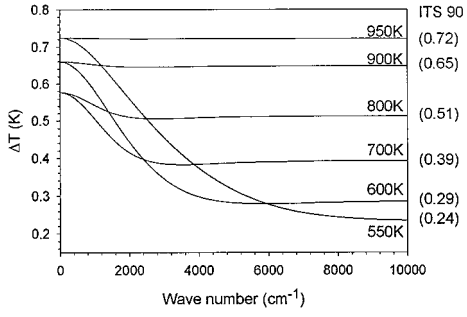


Fig. 4. Uncertainty in the derived temperature from a 0.8-K uncertainty in each reference temperature. The curves were computed at the indicated temperatures for $T_1 = 500$ K and $T_2 = 1000$ K. See the text for an explanation of the values at the right of the graph.

the limiting linear temperature form of Planck's law, $L = (c_1/c_2)\nu^2 T$, for low-wave-number values. In this spectral range ($c_2\sigma \ll T_1$) Eq. (5) approaches a linear temperature interpolation scheme. For temperatures close to the reference temperatures, a maximum uncertainty is reached that is nearly equal to the uncertainty in the reference point itself. The behavior between these two extremities is a smooth, primarily decreasing, function of frequency.

From Fig. 4, the reference uncertainty contribution is currently in the 0.25–0.7-K range and is believed to be a significant component of the total uncertainty. As we have neglected the blackbody temperature nonuniformity, this range probably underestimates the total source-related uncertainty component.

From the interpolation formula [Eq. (5)] it can be seen that an error in the reference temperatures will lead to a systematic change of the interpolated radiance. For example, if the measured $T_2$ is too high, the whole radiance curve increases, and the derived temperature is too large at all frequencies. The uncertainty in the interpolated temperature is therefore expected to be frequency correlated, and averaging the temperature curve cannot be expected to reduce the uncertainty much.

A precision-controlled high-uniformity large-aperture blackbody source is currently being constructed in our laboratory to bring the reference point uncertainty into the 1–15-mK range, permitting an accurate study of the voltage ratio measurement uncertainty.

The uncertainty components in the voltage ratio are the most important quantities that we have to consider because they are fundamental to the technique. The voltage ratio will have uncertainty components from the frequency shift caused by the finite detection solid angle, the detector nonlinearity, the interferometer instability, background changes, wave-number inaccuracy, and finite resolution. In some cases, such as for the solid-angle frequency shift, the detector nonlinearity, and the finite resolution, it may be possible to apply a correction to the voltage ratio, thereby reducing the uncertainty.

The first source of uncertainty in the voltage ratio that we consider is the short-time signal instability of the interferometer and the detector noise. We obtained this information by acquiring a set of 256 spectra, each as a single scan; the entire set was collected over 15 min. We then used this set to compute the standard deviation and the deviation of the mean. This computation can be done directly either on the interferogram or on the spectrum, although the information obtained from the two is slightly different: Because each interferogram is individually Fourier-transform and phase corrected, the computed standard deviation in frequency space does not have any contribution from slow phase drifts.

A typical result for the interferogram is shown in Fig. 5(a), where the standard deviation is plotted versus path difference. Most of the deviation is near the zero path-difference point. The double-peaked structure indicates that the source of uncertainty is

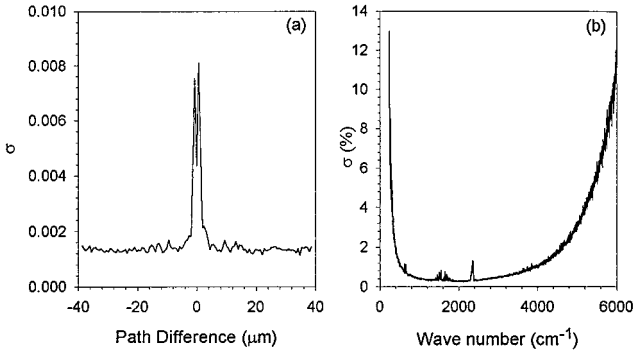


Fig. 5. Standard deviation for 256 single-scan experiments for (a) the interferogram and (b) the spectrum.

linked to the slope of the interferogram, pointing to phase drift errors. The mechanism that generates this phase noise remains to be identified. Assuming the phase drift to be slow on the scale of a single scan acquisition, we can make an estimate of the effect of this phase drift on the Fourier-transform spectra by computing the difference between the Fourier transform of the coadded interferograms and the coadded phase corrected spectra:

$$\frac{\Delta V}{V} = \exp(-2\pi^2\nu^2\langle\varepsilon^2\rangle) - 1, \tag{11}$$

where $\langle\varepsilon^2\rangle$ is the average of the squared path-difference drift. At 2000 $cm^{-1}$ and for a typical drift of 10 nm, the relative spectrum uncertainty is 0.002%. As we shall see shortly, this is at least a factor of 10 lower than the effect observed in the frequency domain.

In the frequency domain the interferometer satisfies the manufacturer's specification of 0.2% standard deviation at 2000 $cm^{-1}$ [Fig. 5(b)] for the highest-temperature spectra. More important for us, the deviation of the mean can be interpreted as a component of the measured voltage absolute uncertainty. As we typically perform 256 scans, this contribution is simply the standard deviation curve of Fig. 5(b) scaled down by a factor of 16 (i.e., $\sqrt{N}$ scans), assuming a Poisson distribution. It should be noted that the measurement has a contribution from the long-term drift, so the calculated uncertainty could be seen as an upper bound on the random signal variations. From relation (4), $\Delta r$ is related to these single voltage measurement uncertainties by the following equation:

$$\Delta r = r\left\{\left(\frac{\Delta V}{V - V_1}\right)^2 + \left[\frac{V_2 - V}{(V_2 - V_1)(V - V_1)}\,\Delta V_1\right]^2 + \left(\frac{\Delta V_2}{V_2 - V_1}\right)^2\right\}^{1/2}. \tag{12}$$

As for $r$, the voltage differences in Eq. (12) are to be computed by use of the interferograms. For the present signal level, the absolute voltage uncertainty depends very little on the radiance: The absolute

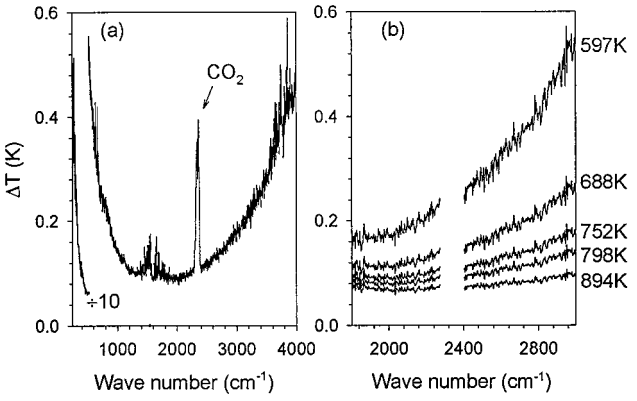


Fig. 6. (a) Estimated uncertainty in the temperature caused by the signal reproducibility for the 752-K spectrum, (b) frequency range with minimal temperature uncertainty for different temperatures. The $CO_2$ peaks near 2350 $cm^{-1}$ are not shown.

standard deviation curves for a room-temperature blackbody and the 1000-K blackbody are virtually identical. In such a case, noting that $V - V_1 = r(V_2 - V_1)$ and that $(1 - r) = (V_2 - V)/(V_2 - V_1)$, we can simplify Eq. (12) to

$$\Delta r = [1 + (1 - r)^2 + r^2]^{1/2} \frac{\Delta V}{V_2 - V_1}. \quad (13)$$

Furthermore, the pre-factor of $\Delta V/(V_2 - V_1)$ is typically between 1.2 and 1.4 for the covered temperature and frequency range. The result for the uncertainty in $r$, $\Delta r$, is therefore close to that already presented for $\Delta V/V$.

Combining Eqs. (7), (10), and (13) transforms the uncertainty in the voltage ratio into the uncertainty in the temperature, as presented in Fig. 6(a). The uncertainty in the temperature takes its minimum value near 2000 $cm^{-1}$, where the spectrometer has optimal sensitivity, and it has values ranging from 0.06 to 0.16 K [Fig. 6(b)] for a 256-scan experiment. $CO_2$ concentration variability in the unpurged section of the optical path is responsible for the large increases in the temperature uncertainty between 2300 and 2400 $cm^{-1}$. The uncertainty level rises rapidly near the low-frequency limit of the spectrum to reach values larger than 10 K below 250 $cm^{-1}$.

The temperature uncertainty is consistent with the observed noise on the temperature curve and comes mostly from the detector noise. A weighted average of the temperature curve (≈2000 points) is therefore expected to reduce this uncertainty component by a substantial factor. So, as long as we restrict the measurement to a range of wave-number where the irreproducibility is low, this contribution to the temperature uncertainty is small, because the source temperature uncertainty dominates.

A second uncertainty component in the voltage ratio comes from the finite resolution. The interferograms are measured only for finite path difference, and when the Fourier transform is performed this leads to the convolution of the ideal spectrum with an instrumental line shape. The effect was discussed by Yu *et al.*,[5] and their approximate correction can be written as

$$\Delta r = -\frac{1}{6}\left(\frac{1}{2X}\right)^2 \left\{ r'' + 2r' \left[ \frac{(L_2 - L_1)'}{L_2 - L_1} + \frac{R'}{R} \right] \right\}, \quad (14)$$

where $X$ is the scanning length and the primes indicate wave-number derivatives. $R$ is the interferometer response of Eq. (3). Because this is a small correction, the second derivative of the voltage ratio can be computed from the defining expression with the best estimate of the unknown temperature, in this way avoiding the noisy second derivative of experimental quantities. If necessary, this process can be iterated.

From Eq. (14), the effect is of the order of 3 parts in $10^7$ near 2700 $cm^{-1}$, approximately 1000 times smaller than the effect of the interferometer instability. Therefore it will become necessary to apply a correction for this effect as the uncertainty level on the measurement approaches 1 mK. Alternatively, the resolution could be increased to decrease further the correction magnitude.

A third effect on the voltage ratio that should be considered and corrected for is the detector nonlinearity. Even though detector-specific corrections[17] can be developed when the origin of the nonlinearity is well understood, we are unaware of any general, high-accuracy correction method in Fourier-transform infrared (FT-IR) spectroscopy, such as the radiance summation approach[18–20] used in conventional radiometry. The design of a nonlinearity correction for use in Fourier-transform spectroscopy is complicated by the presence of the unmeasured incoherent signal component (dc signal component). For those detectors that respond to unmodulated radiation, such as InSb, it should be a relatively simple matter to adapt the radiance summation technique. For detectors without a dc response, such as our current DTGS detector, it seems difficult to avoid a measurement of the interferometer's modulation efficiency. Without such a measurement it is impossible to estimate accurately the total power falling onto the detector and therefore to determine the appropriate correction factors. The subject of nonlinearity correction in FT-IR spectroscopy remains an open one. It should be emphasized that simple removal of the out-of-band signal through deconvolution, as proposed by Sakhnovskii and Timochko,[21] will not produce the desired linearization; a term that is quadratic in the total power falling upon the detector involves not only the square of the modulated intensity but also the product of the dc term and the modulated part. The last term gives rise to an intensity-dependent rescaling of the interferogram (and therefore has no out-of-band effect) that is larger than the square of the modulated component because the modulation efficiency is less than unity.

Our preliminary attempt to check the linearity *in situ*, using the interferometer and a two-aperture method, led to nonlinearity ratios[18] that vary ran-

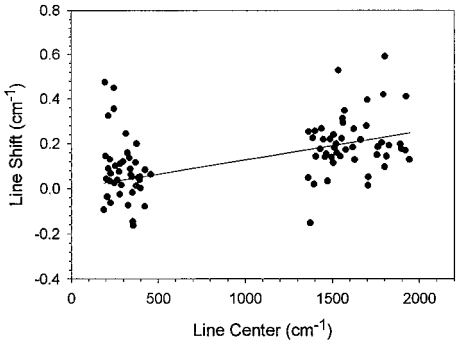


Fig. 7. Difference between the measured values and literature values of water absorption bands as a function of line frequency. Solid curve, best fit to the expected straight line with the equation $\Delta\nu = 1.3 \times 10^{-4}\nu$.

domly from 0.997 to 1.003. We believe, however, that because the measurements were acquired over a period of a few hours, the dominant factor in the 0.3% fluctuations is the interferometer drift rather than the intrinsic detector nonlinearity that we were trying to measure. This conclusion illustrates the nature of the experimental complications that can arise during any attempt to quantify nonlinearity in a Fourier-transform system.

The long-term stability of the interferometer is also an important issue. By long term we mean the period necessary to acquire the references and unknown temperature spectra (typically several hours with our current setup). Given the accuracy level that we want to achieve, interferometer temperature drift caused by room-temperature changes should be avoided. There are several quantities that can exhibit thermal drift. The DTGS detector is a thermal detector, and a change of 1 K in room temperature can change the detector response by as much as 0.5%.[22] The effect of beamsplitter temperature changes on the FT-IR signal have also been reported to be near 1%/K.[22] Changes in the spectra at the 0.2–0.5% level are regularly encountered in long-term (~10-h) measurements, which translate into uncertainties of the order of 0.5–2 K in the interpolated temperature at 2000 cm$^{-1}$.

The last source of uncertainty explored experimentally relates to the finite solid angle: In interferometric systems, shorter optical path differences are introduced for off-axis rays, and this leads to a redshift of the observed spectra.[3] We obtained the magnitude of this effect for our system by measuring water-vapor absorption bands, fitting the absorbance with a sum of Lorentzian line shapes, and comparing the result with a table of water lines.[23] The results are shown in Fig. 7. The observed line shift agrees well with the shift expected from the $\Omega = 2 \times 10^{-3}$ sr detector-limited solid angle $\{\Delta\nu = [\Omega/(4\pi)]\nu = 1.6 \times 10^{-4}\nu\}$. The uncertainty in the lines' positions is seen to be 2 parts in $10^4$, and this leads to a calculated temperature uncertainty of the order of 25 mK. Rescaling the wave-number axis according to the measured coefficient can reduce this uncertainty component further.

There are a few other sources of uncertainty that have not been seriously addressed experimentally. Most of these are believed to be smaller and hidden by the current sources of uncertainty. One such uncertainty component is the variation in blackbody emissivity with temperature: Because of the ratio in relation (4) and the experimental use of a single variable-temperature blackbody source, there is no uncertainty introduced in the temperature by the use of a graybody that has a temperature-independent emissivity less than unity.

Source uniformity, beam uniformity, detector uniformity, and diffraction are other effects that remain to be explored.

It should be noted that it is still generally possible to apply relation (4) and Eqs. (5) and (6) in situations that involve a small correction to the measured voltages. For example, if three blackbodies of known emissivity are being used (or, generally, any known multiplicative correction to the radiance is present) the measured voltage ratio will be related to the radiance by

$$r_m = \frac{\varepsilon L - \varepsilon_1 L_1}{\varepsilon_2 L_2 - \varepsilon_1 L_1}. \tag{15}$$

By substituting into Eq. (15) the left-hand side of Eq. (5) for $L$, it is straightforward to isolate the radiance ratio $r$, now including the effect of emissivities explicitly:

$$r = \frac{(\varepsilon_2 L_2 - \varepsilon_1 L_1)}{\varepsilon(L_2 - L_1)} r_m + \frac{(\varepsilon_1 - \varepsilon)L_1}{\varepsilon(L_2 - L_1)}. \tag{16}$$

Inasmuch as all the components of the slope and the offset terms are known, Eq. (16) provides a means to correct the measured voltage ratio $r_m$ for deviations from the ideal (blackbody) case given by relation (4). From Eq. (16), the uncertainty on the (corrected) voltage ratio caused by an uncertainty on the emissivities is given by

$$\Delta r = \left\{ \left[ \frac{(1 - r_m)\varepsilon_1 L_1}{\varepsilon L} \frac{\Delta\varepsilon_1}{\varepsilon_1} \right]^2 + \left( \frac{r_m \varepsilon_2 L_2}{\varepsilon L} \frac{\Delta\varepsilon_2}{\varepsilon_2} \right)^2 + \left( \frac{\Delta\varepsilon}{\varepsilon} \right)^2 \right\}^{0.5} \frac{L}{L_2 - L_1}, \tag{17}$$

so, in the case when Eq. (5) is used for interpolation,

$$\Delta T \leq \frac{T^2}{c_2 \nu} \left[ 1 - \exp\left( -\frac{c_2 \nu}{T} \right) \right] \left[ \left( \frac{\Delta\varepsilon_1}{\varepsilon_1} \right)^2 + \left( \frac{\Delta\varepsilon_2}{\varepsilon_2} \right)^2 + \left( \frac{\Delta\varepsilon}{\varepsilon} \right)^2 \right]^{1/2}. \tag{18}$$

Inequality (18) implies that to achieve an accuracy of 100 mK at a temperature of 1000 K and a frequency of 2600 cm$^{-1}$ one must know the emissivities to 2 parts in $10^4$.

One can also apply Eq. (16), if the two reference blackbodies have known emissivities but the unknown temperature object has an unknown emissivity, by setting $\varepsilon = 1$. In this case Eq. (5) can be used as an interpolation formula for a general (nonblack-

Table 1. Temperature-Uncertainty Components at 2700 $cm^{-1}$ versus Observed Temperature

| Uncertainty Component | Observed Temperature (K)[a] 598.0 (597.4) | 689.4 (688.2) | 752.3 (751.9) | 798.3 (798.2) | 894.4 (894.2) |
|---|---|---|---|---|---|
| Low-temperature reference (0.8 K) | 0.3 | 0.1 | 0.09 | 0.07 | 0.03 |
| High-temperature reference (0.8 K) | 0.2 | 0.4 | 0.4 | 0.5 | 0.6 |
| Long-term drift (0.5%) | 0.6 | 0.8 | 0.9 | 1.0 | 1.3 |
| Stability and detector noise | 0.3 | 0.2 | 0.1 | 0.1 | 0.08 |
| Nonlinearity (0.05%) | 0.06 | 0.08 | 0.09 | 0.1 | 0.1 |
| Finite solid angle | 0.02 | 0.03 | 0.02 | 0.02 | 0.01 |
| Finite resolution (4 $cm^{-1}$) | 0.0003 | 0.0003 | 0.0002 | 0.0002 | 0.0001 |
| Combined uncertainty | 0.8 | 0.9 | 1.0 | 1.1 | 1.4 |

[a]The thermocouple temperature reading is indicated in parentheses.

body) radiance, but Eqs. (6) and (7) can no longer be used. A different approach, such as fitting the radiance to a model, must be used to extract the temperature and its uncertainty. As a particular case, if the emissivity of the body under investigation is known to be gray (i.e., independent of wavelength) over some spectral band, curve fitting can be applied to the radiance in this band to extract the temperature and the (single parameter) emissivity; once the temperature is known, the (frequency-dependent) emissivity can be obtained over the entire measured spectral region by application of Eq. (2). Table 1 summarizes the temperature-uncertainty components at 2700 $cm^{-1}$ and for reference temperatures of 492.8 and 1000.0 K.

## 5. Conclusions

An interpolation technique for temperature measurement in the 500–1000-K range with a Fourier-transform spectrometer was described. A set of measurements was presented and the sources of uncertainties analyzed. The present temperature accuracy is below 2 K. The main uncertainty components are the imprecise blackbody reference temperatures (0.4–0.7 K) and the interferometer thermal instability (0.7–1.3 K). A reduction of these uncertainty components is the next step of our investigation.

Once the new apparatus is in place, the uncertainty level is expected to decrease by a factor of 20. Near the 0.1-K uncertainty level the low-sensitivity DTGS noise could become a problem. It would then be necessary to select a detector with a higher $D^*$, such as InSb or HgCdTe, which has the disadvantage of significantly larger nonlinearity. The development of an accurate nonlinearity-correction procedure for use in Fourier-transform radiometry is expected to become one of the outstanding issues.

The authors thank Ron Bedford for useful discussions and critical reading of the manuscript. Don Woods and Erroll Murdock are also thanked for their skilled technical assistance. Finally, Pierre C. Dufour acknowledges NRC/NSERC for support in the form of a postdoctoral grant from the National Research Council–National Science and Engineering Research Council.

## References

1. T. J. Quinn and J. E. Martin, "Cryogenic radiometry, prospects for further improvements in accuracy," Metrologia **28,** 155–161 (1991).
2. C. C. Hoyt and P. V. Foukal, "Cryogenic radiometers and their application to metrology," Metrologia **28,** 163–167 (1991).
3. J. Chamberlain, *The Principles of Interferometric Spectroscopy* (Wiley, Chichester, UK, 1979), Chap. 1, pp. 15–18; Chap. 8, pp. 221–224.
4. H. E. Revercomb, H. Buijs, H. B. Howell, D. D. LaPorte, W. L. Smith, and L. A. Sromovsky, "Radiometric calibration of IR Fourier transform spectrometers: solution to a problem with the High-Resolution Interferometer sounder," Appl. Opt. **27,** 3210–3218 (1988).
5. M. Yu. Sakhnovskii, B. M. Timochko, V. B. Karavanov, M. G. Kunetskii, V. A. Novoselov, and E. I. Aleshko, "Fourier-radiometric method for determining the spectra, emissivity, and temperature of bodies," Opt. Spectrosc. (USSR) **71,** 468–470 (1991).
6. E. Lindermeir and V. Tank, "The spectral emissivity of natural surfaces measured with a Fourier transform infrared spectrometer," Measurement **14,** 177–187 (1994).
7. S. Clausen, A. Morgenstjerne, and O. Rathmann, "Measurement of surface temperature and emissivity by a multitemperature method for Fourier-transform infrared spectrometers," Appl. Opt. **35,** 5683–5691 (1996).
8. P. Haschberger and E. Lindermeir, "Spectrometric inflight measurement of aircraft exhaust emissions: first results of the June 1995 campaign," J. Geophys. Res. **101,** 25,995–26,006 (1996).
9. P. Gori Giorgi, "Influence of the angular response on Fourier absolute spectrometry the case of COBE-FIRAS," Infrared Phys. Technol. **36,** 749–753 (1995).
10. S. Clausen and L. H. Sørensen, "Measurement of single moving particle temperatures with an FT-IR spectrometer," Appl. Spectrosc. **50,** 1103–1111 (1996).
11. E. Lindermeir, P. Haschberger, V. Tank, and H. Dietl, "Calibration of a Fourier transform spectrometer using three blackbody sources," Appl. Opt. **31,** 4527–4533 (1992).
12. H. A. Gebbie, R. A. Bohlander, and R. P. Futrelle, "Properties of photons determined by interferometric spectroscopy," Nature (London) **240,** 391–394 (1972).
13. H. A. Gebbie, "Quantum based temperature standards," Infrared Phys. **34,** 575–577 (1993).
14. H. Preston-Thomas, "The International Temperature Scale of 1990 (ITS-90)," Metrologia **27,** 3–10 (1990).
15. J. M. Palmer, "The measurement of transmission, absorption,

emission, and reflection," in *Handbook of Optics, Devices, Measurements, & Properties*, 2nd ed., M. Bass, ed. (McGraw-Hill, New York, 1995), Vol. 2, Chap. 25, p. 25.7.
16. *Supplementary Information for the International Temperature Scale of 1990* (Bureau International des Poids et Mesures, Sèvres, France, 1990).
17. K. Rahmelow, "Electronic influences on an infrared detector signal: nonlinearity and amplification," Appl. Opt. **36,** 2123–2132 (1997).
18. E. F. Zalewski, "Radiometry and photometry," in *Handbook of Optics, Devices, Measurements, & Properties*, 2nd ed., M. Bass, ed. (McGraw-Hill, New York, 1995), Vol. 2, Chap. 24, p.24.38.
19. W. Budde, "Multidecade linearity measurements on Si photodiodes," Appl. Opt. **18,** 1555–1558 (1979).
20. L. Coslovi and F. Righini, "Fast determination of the nonlinearity of photodetectors," Appl. Opt. **19,** 3200–3203 (1980).
21. M. Yu. Sakhnovskii and B. M. Timochko, "Nonlinearity of the photoreceiving channel of the Fourier spectrometer and the method for compensating it," Opt. Spectrosc. **79,** 647–649 (1995).
22. D. M. MacBride, C. G. Malone, J. P. Hebb and E. G. Cravalho, "Effect of temperature variation on FT-IR spectrometer stability," Appl. Spectrosc. **51,** 43–50 (1997).
23. J.-M. Flaud, C. Camy-Peyret, and R. A. Toth, *Selected Constants: Water Vapor Line Parameters from Microwave to Medium Infrared* (Pergamon, Oxford, 1981).